Plasma Science and Technology

PAPER

Diffusion of ions in an electrostatic stochastic field and a space-dependent unperturbed magnetic field

To cite this article: Marian NEGREA 2020 *Plasma Sci. Technol.* **22** 015101

Plasma Sci. Technol. **22** (2020) 015101 (14pp) https://doi.org/10.1088/2058-6272/ab491e

Diffusion of ions in an electrostatic stochastic field and a space-dependent unperturbed magnetic field

Marian NEGREA

Department of Physics Association Euratom-MEdC, Romania University of Craiova, A.I.Cuza str.13, 200585 Craiova, Romania

E-mail: mnegrea@yahoo.com

Received 18 July 2019, revised 30 September 2019
Accepted for publication 30 September 2019
Published 1 November 2019

Abstract

We calculate the diffusion coefficients for ions moving in a prescribed electromagnetic field. The field is considered to be a superposition of an electrostatic stochastic field and a space-dependent and sheared magnetic field. We have considered as parameters involved in the calculation of the diffusion coefficients the shear ion Kubo number K_s^{ion}, the electrostatic Kubo number K, the parallel shear ion Kubo number K_{zs}^{ion}, and the parallel thermal ion Kubo number K_z^{ion}. A geometrical parameter which is the measure of the product of the stochastic perpendicular correlation length and the gradient in the magnetic field strength (see definitions in the text) is found not to be important in our calculation. The results concerning the diffusion coefficients obtained in our model are in agreement with experimental data and with those corresponding to other models, and the neoclassical and anomalous values for the diffusion coefficients are obtained.

Keywords: magnetic field, turbulence, diffusion

(Some figures may appear in colour only in the online journal)

1. Introduction

Transport of particles in fusion plasma is still a very important issue for researchers. The theoretical results obtained for the transport coefficients from classical transport theory (see e.g. [1]) are not in agreement with the experimental results. The agreement is improved if the geometry of the magnetic field is taken into account for the calculation of the transport coefficients and the neoclassical transport theory is built (see e.g. [2] and [3]). Even neoclassical theory cannot explain some aspects of the diffusion of particles in a chaotic (turbulent) plasma. In this kind of plasma, transport is called anomalous if turbulence dominates the classical and neoclassical contributions to transport. The approximation that treated trapping in a new manner compared with the papers of Isichenko M B [4, 5], the numerical treatment given in [6] and [7] and used also in our paper to calculate the diffusion coefficients is the decorrelation trajectory method (DCT). There exist also a large amount of experimental, theoretical, and numerical papers (see, for example, references [8–26]) that are dedicated to the understanding and control of transport in magnetically confined plasmas. The DCT is presented in the following selection of papers [8, 9, 11, 14, 22, 23].

Results concerning the radial flux of particles obtained in reference [24] were used in order to calculate the effect of parallel fluctuations; in our paper only the perpendicular fluctuations (to the mean magnetic field) are taken into account. Separation of magnetic field lines, which is important for the calculation of diffusion coefficients, has been studied in many papers; see reference [25] and citations within. Particle behavior is a complex problem related to the confinement and transport of the bulk ions and electrons in plasma and to the plasma–wall interaction. This is a very important issue for the development of fusion reactors.

Our paper studied the problem of the diffusion of ions in a space-dependent magnetic field and a divergenceless electrostatic stochastic field. The shape of the diffusion coefficients of a particle moving in a magnetic field with shear

combined with an electrostatic stochastic field has been studied in many papers (see e.g. [27]). Numerical studies (such as 'direct numerical simulations') are devoted to the transport of particles in such a combination of fields (see e.g. [28]). All these issues are presented in the very good book of Radu Balescu [29]. Our theoretical results are in agreement with the experimental ones. In our paper the magnetic field is dependent on the radial coordinate and the electrostatic stochastic field influences the values of the diffusion coefficients. The movement of particles was analyzed also in a guiding center model with a stochastic anisotropic magnetic field [30]. The results concerning the diffusion coefficients are similar with those obtained in the present paper. The conclusion is that, at least from these two different physical models, practically we obtained the same diffusion coefficient behavior. In our paper we will use some results obtained in reference [8], and the paper is organized as follows. The magnetic field model and the approximate guiding center equations are established in section 2. In section 3, some details of the DCT approach are presented and the necessary Eulerian correlations are derived using a standard procedure of the DCT method. We have also defined here the parameters (specific to the ions) involved in the change of the diffusion coefficients, namely the ion shear Kubo number $K_{\rm s}^{\rm ion}$, the electrostatic ion Kubo number $K^{\rm ion}$, parallel shear ion Kubo number $K_{\rm zs}^{\rm ion}$, the parallel thermal ion Kubo number $K^{\rm ion}$ and the geometrical parameter α_R, which is the measure of the product of the stochastic perpendicular correlation length and the gradient in the magnetic field strength. Here the specific parameters of the motion of ions are defined. Before the section 4 we introduce some comments on the issues related to Kubo numbers, trapping and the open trajectories. In section 4 we calculate the diffusion coefficients and averaged global velocities. We also calculate the trapping time for different values of the parameters. The conclusions are provided in section 5.

2. The magnetic field model and the approximate guiding center equations

In our paper we consider that particles are moving in an electrostatic stochastic electric field combined with a magnetic field that is unperturbed and has the form

$$\mathbf{B} = B_0[b(X)\mathbf{e}_z + s(X)\mathbf{e}_y] \tag{1}$$

where $s(X) \equiv XL_{\rm s}^{-1}$ with $L_{\rm s}$ the shear length and the z component, i.e. $\mathbf{B}_z$ that depends on the radial coordinate X and has the form $\mathbf{B}_z = B_0(1 + X/R)^{-1}\mathbf{e}_z$ with $1/R$ representing the gradient in the magnetic field strength (density of magnetic field lines) in the Ox direction.

The guiding center trajectories are determined from the approximate equations

$$\frac{{\rm d}\mathbf{R}}{{\rm d}t} \simeq U\mathbf{b} + \frac{\mathbf{E}\times\mathbf{B}}{B^2},\ \ \mathbf{R} \equiv (\mathbf{X}, Z),\ \ \mathbf{X} \equiv (X, Y) \tag{2}$$

where U is the parallel velocity, which we will approximate here with the thermal one, i.e. $V_{\rm th}$. In order to make the system dimensionless we introduce the typical correlation lengths: $\lambda_\perp$ is the perpendicular correlation length and $\lambda_\parallel$ is the parallel correlation length along the main magnetic field. $\tau_{\rm c}$ is the correlation time of the fluctuating electrostatic field and ε is a measure of the amplitude of the electrostatic field fluctuations. The correlation time $\tau_{\rm c}$ is the maximum time interval over which the field (the electrostatic potential in our case) maintains a given structure and is about 10^{-5} s, the perpendicular correlation length $\lambda_\perp$ is about 10^{-2} m as was observed by several plasma turbulence diagnostics looking at the edge region of the tokamaks [31, 32] and $\lambda_\parallel$ is about 1–10 m. Using the results obtained in [8] and the dimensionless quantities x, y, z, τ and φ defined as

$$\mathbf{x} = \frac{\mathbf{X}}{\lambda_\perp};\ \ z = \frac{Z}{\lambda_\parallel};\ \ \tau = \frac{t}{\tau_{\rm c}};\ \ \Phi(\mathbf{X}, t) = \varepsilon\varphi\left(\frac{\mathbf{X}}{\lambda_\perp}, \frac{Z}{\lambda_\parallel}, \frac{t}{\tau_{\rm c}}\right) \tag{3}$$

we obtain the following dimensionless Langevin system of equations [8]:

$$\frac{{\rm d}x}{{\rm d}\tau} = -K(1 + \alpha_R x)\frac{\partial\varphi}{\partial y} \tag{4}$$

$$\frac{{\rm d}y}{{\rm d}\tau} = K(1 + \alpha_R x)\frac{\partial\varphi}{\partial x} + K^{\rm ion}x \tag{5}$$

$$\frac{{\rm d}z}{{\rm d}\tau} = K_{\rm zs}x\frac{\partial\varphi}{\partial x} + K_z b^{-1}(\alpha_R x). \tag{6}$$

We write here the different Kubo numbers already defined in [8] entering the system of equations given in (4)–(6):

$$K = \frac{\varepsilon\tau_{\rm c}}{B_0\lambda_\perp^2} \tag{7}$$

is the electrostatic Kubo number

$$K_{\rm s} = \frac{\tau_{\rm c}V_{\rm th}}{L_{\rm s}} \tag{8}$$

is the shear Kubo number

$$K_{\rm zs} = \frac{\varepsilon\tau_{\rm c}}{B_0\lambda_\parallel L_{\rm s}} \equiv K\frac{\lambda_\perp^2}{\lambda_\parallel L_{\rm s}} \tag{9}$$

is the parallel shear Kubo number and

$$K_z = \frac{V_{\rm th}\tau_{\rm c}}{\lambda_\parallel} \tag{10}$$

is the parallel thermal Kubo number. The geometrical parameter α_R is defined as the product of the stochastic perpendicular correlation length and the gradient in the magnetic field strength

$$\alpha_R = \lambda_\perp/R. \tag{11}$$

Considering that the thermal velocity used in the former expressions corresponds to ions, the following corresponding Kubo numbers for ions can be defined:

$$K_{\rm s}^{\rm ion} = \frac{\tau_{\rm c}(V_{\rm th})^{\rm ion}}{L_{\rm s}} \tag{12}$$

$$K_{zs}^{ion} = \frac{(V_{th})^{ion}\tau_c}{\lambda_{\parallel}}. \quad (13)$$

3. Details of the DCT approach

From the orders of magnitude of the different Kubo numbers given in [8] we can suppose that the term containing K_{zs}^{ion} can be neglected in the equation (6). We also suppose that

$$K_z^{ion}(1 + x\lambda_\perp/R) \simeq K_z^{ion}$$

because $K_z^{ion} \in [10^{-3}, 1]$ and $x\lambda_\perp/R \approx 10^{-2}$. In this case the equation (6) becomes deterministic with the solution

$$z = \frac{V_{th}\tau_c}{\lambda_{\parallel}}\tau + z(0) \quad (14)$$

where we can choose $z(0) = 0$. An implicit dependence on time appears in the potential and the Langevin system of equations given in (4)–(6) becomes a 2D system

$$\frac{dx}{d\tau} = -Kb^{-1}(x\lambda_\perp/R)\frac{\partial\varphi\left(x, y, \frac{V_{th}\tau_c}{\lambda_{\parallel}}\tau, \tau\right)}{\partial y}$$
$$\frac{dy}{d\tau} = Kb^{-1}(x\lambda_\perp/R)\frac{\partial\varphi\left(x, y, \frac{V_{th}\tau_c}{\lambda_{\parallel}}\tau, \tau\right)}{\partial x} + K_s^{ion}x. \quad (15)$$

For this system the DCT method can be applied in order to calculate the diffusion coefficient and other quantities of interest. For the stochastic dimensionless electrostatic potential $\varphi(\mathbf{x}, z, \tau)$ we can choose the following spatiotemporal autocorrelation

$$C(\mathbf{x}; z, \tau) = \langle\varphi(\mathbf{0}, 0, 0)\varphi(\mathbf{x}, z, \tau)\rangle = A(\mathbf{x})E_2(z)T(\tau) \equiv A(\mathbf{x})B(\tau)$$

where

$$A(\mathbf{x}) = \exp(-\mathbf{x}^2/2), \quad E_2(z) = \exp(-|z|) \quad (16)$$

and

$$T(\tau) = \exp(-\tau), \quad \tau \geqslant 0. \quad (17)$$

If we use solution (14), the function $B(\tau)$ becomes

$$B(\tau) \equiv E_2(z)T(\tau) = \exp(-|z| - \tau) = \exp\left[-\left(\frac{V_{th}\tau_c}{\lambda_{\parallel}} + 1\right)\tau\right] \equiv \exp[-(K_z^{ion} + 1)\tau] \quad (18)$$

where definition (13) was used.

The autocorrelation becomes

$$C(\mathbf{x}, \tau) \equiv A(\mathbf{x})B(\tau) = \exp(-\mathbf{x}^2/2)\exp[-(K_z^{ion} + 1)\tau]. \quad (19)$$

The statistical properties of all the fluctuating quantities are calculated by taking appropriate derivatives of equations (16) and (17). We introduce the notations for the 'directly fluctuating velocities' as

$$v_x = -\frac{\partial\varphi}{\partial y}; \; v_y = \frac{\partial\varphi}{\partial x}. \quad (20)$$

From equation (19), we can deduce the Eulerian correlations between the directly fluctuating velocities C_{ij} $(i, j = x, y)$ and the mixed correlations $C_{\varphi i}$ $(i = x, y)$ using the standard procedure given in [9–11]:

$$C_{xx}(\mathbf{x}, \tau) = -\frac{\partial^2 C(\mathbf{x}, \tau)}{\partial y^2} = (1 - y^2)C(\mathbf{x}, \tau)$$
$$C_{yy}(\mathbf{x}, \tau) = -\frac{\partial^2 C(\mathbf{x}, \tau)}{\partial x^2} = (1 - x^2)C(\mathbf{x}, \tau) \quad (21)$$

$$C_{xy}(\mathbf{x}, \tau) = C_{yx}(\mathbf{x}, \tau) = \frac{\partial^2 C(\mathbf{x}, \tau)}{\partial x\partial y} = x\, y\, C(\mathbf{x}, \tau) \quad (22)$$

$$C_{x\varphi}(\mathbf{x}, \tau) = -C_{\varphi x}(\mathbf{x}, \tau) = \frac{\partial C(\mathbf{x}, \tau)}{\partial y} = -y\, C(\mathbf{x}, \tau)$$
$$C_{y\varphi}(\mathbf{x}, \tau) = -C_{\varphi y}(\mathbf{x}, \tau) = -\frac{\partial C(\mathbf{x}, \tau)}{\partial x} = x\, C(\mathbf{x}, \tau) \quad (23)$$

where the following general relations were used:

$$\langle\varphi(\mathbf{0}, 0)v_j(\mathbf{x}, \tau)\rangle = C_{\varphi j}(\mathbf{x})B(\tau);$$
$$\langle v_i(\mathbf{0}, 0)v_j(\mathbf{x}, \tau)\rangle = C_{ij}(\mathbf{x})B(\tau); \;\; i, j = x, y \quad (24)$$

$$C_{ij}(\mathbf{x}) = -\varepsilon_{in}\varepsilon_{jp}\frac{\partial^2 A(\mathbf{x})}{\partial x_n\partial x_p};$$

$$C_{\varphi i}(\mathbf{x}) = -C_{i\varphi}(\mathbf{x}) = -\varepsilon_{in}\frac{\partial A(\mathbf{x})}{\partial x_n}; \;\; i, j, p, n = x, y \quad (25)$$

and also the antisymmetric tensor ε_{ij} ($\varepsilon_{12} = -\varepsilon_{21} = 1$, $\varepsilon_{11} = \varepsilon_{22} = 0$). Using these correlations we can develop the procedure of the DCT needed to calculate the components of the diffusion tensor components specific to our field. We introduce the following change of variable

$$\tau_{ion} \equiv (K_z^{ion} + 1)\tau. \quad (26)$$

With this change of variable system (15) becomes (in the following we will drop the subscript 'ion' from τ_{ion})

$$\frac{dx}{d\tau} = -K^{ion}b^{-1}(x\lambda_\perp/R)\frac{\partial\varphi(x, y, \tau; K_z^{ion})}{\partial y} \equiv K^{ion}b^{-1}(x\lambda_\perp/R)v_x$$
$$\frac{dy}{d\tau} = K^{ion}b^{-1}(x\lambda_\perp/R)\frac{\partial\varphi(x, y, \tau; K_z^{ion})}{\partial x} + K_{zs}^{ion}x \equiv K^{ion}b^{-1}(x\lambda_\perp/R)v_y + K_{zs}^{ion}x \quad (27)$$

where the following definitions are introduced:

$$K^{ion} \equiv \frac{K}{K_z^{ion} + 1} \quad (28)$$

and

$$K_{zs}^{ion} \equiv \frac{K_s^{ion}}{K_z^{ion} + 1}. \quad (29)$$

The expression (29) and the definition given in (9) should not be confused. System (27) is studied using the DCT method. The total ensemble of the realizations of the stochastic system

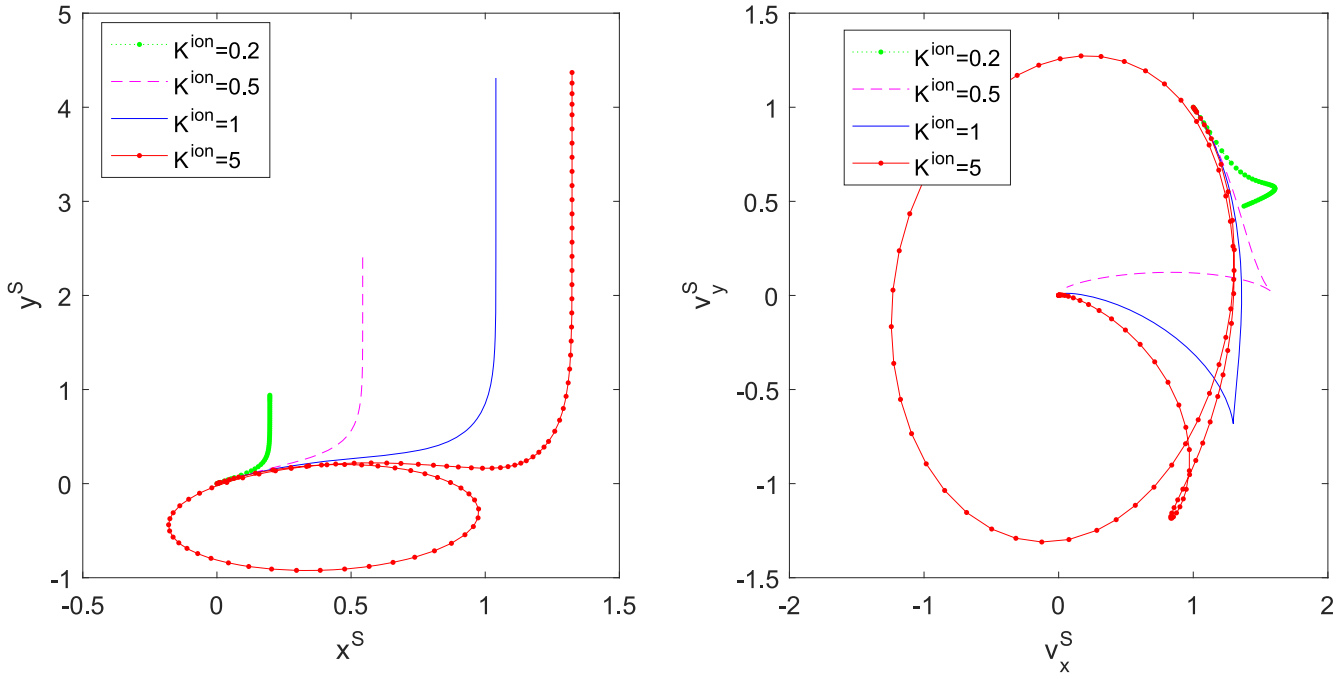

Figure 1. Trajectories and hodographs for $K_s^{\rm ion} = 0.5$, and four values of the level of turbulence in the subensemble given by $\varphi^0 = 2$, $v_x^0 = 1$ and $v_y^0 = 1$.

is a superposition of the subensembles S that are defined by the electrostatic potential φ and the 'directly fluctuating velocities' v_i defined in (20) at time 0, i.e.

$$S:\ \varphi(\mathbf{0}, 0) = \varphi^0, \quad \mathbf{v}(\mathbf{0}, 0) = \mathbf{v}^0. \tag{30}$$

The probability distribution function of these initial values is defined as

$$P_0(\mathbf{v}^0, \varphi^0) = P(v_x^0)P(v_y^0)P(\varphi^0) = (2\pi)^{-\frac{3}{2}} \exp\left\{-\frac{1}{2}[(v_x^0)^2 + (v_y^0)^2 + (\varphi^0)^2]\right\}. \tag{31}$$

The total Lagrangian correlation tensor components of the directly fluctuating velocities appearing in system (27) are

$$L_{ij}(\tau) = \int \mathrm{d}\varphi^0 \mathrm{d}\mathbf{v}^0 P_0(\mathbf{v}^0, \varphi^0) L_{ij}^S(\tau); \quad i, j = x, y \tag{32}$$

where

$$\begin{aligned} L_{ij}^S(\tau) &= \left(\frac{K}{K_z^{\rm ion} + 1}\right)^2 \langle v_i(\mathbf{0}, 0,) v_j[\mathbf{x}(\tau), \tau]\rangle^S \\ &\equiv \left(\frac{K}{K_z^{\rm ion} + 1}\right)^2 v_i^0 \langle v_j[\mathbf{x}(\tau), \tau]\rangle^S \\ &\simeq (K^{\rm ion})^2 v_i^0 v_j^S[\mathbf{x}^S(\tau), \tau] \end{aligned} \tag{33}$$

is the Lagrangian correlation tensor in a subensemble S. and $\langle ...\rangle^S$ denotes the average in the subensemble. The last approximation in (33) is the essence of the DCT method. We have replaced the average velocity in a subensemble with the velocity obtained by using the solutions $\mathbf{x}^S(\tau)$ of the deterministic system given below in equations (37) and (38).

The Eulerian average directly fluctuating velocities $\langle v_j[\mathbf{x}(\tau), \tau]\rangle^S$ in the subensemble S are calculated as

$$\begin{aligned} v_j^S[\mathbf{x}(\tau), \tau] &\equiv \langle v_j[\mathbf{x}(\tau), \tau]\rangle^S = [\varphi^0 C_{\varphi j}(\mathbf{x}) + v_i^0 C_{ij}(\mathbf{x})]B(\tau) \\ &\equiv v_j^S(\mathbf{x})B(\tau) \quad i, j = x, y \end{aligned} \tag{34}$$

and the explicit expressions for $v_j^S(\mathbf{x}, \tau) \equiv v_j^S(\mathbf{x})B(\tau)$ are

$$v_x^S(\mathbf{x})B(\tau) \equiv [v_x^0(1 - y^2) + v_y^0 xy + \varphi^0 y]C(\mathbf{x}, \tau) \tag{35}$$

$$v_y^S(\mathbf{x})B(\tau) \equiv [v_x^0 xy + v_y^0(1 - x^2) - \varphi^0 x]C(\mathbf{x}, \tau). \tag{36}$$

Next, we define, in a subensemble S, a deterministic trajectory by the following equations of motion:

$$\begin{aligned} \frac{\mathrm{d}x^S(\tau)}{\mathrm{d}\tau} &= K^{\rm ion} b^{-1}(x^S(\tau)\lambda_\perp/R) v_x^S(\mathbf{x}^S(\tau))B(\tau) \\ &\equiv w_x^S(\mathbf{x}^S(\tau), \tau) \end{aligned} \tag{37}$$

$$\begin{aligned} \frac{\mathrm{d}y^S(\tau)}{\mathrm{d}\tau} &= x^S(\tau)K_{zs}^{\rm ion} + K^{\rm ion} b^{-1}(x^S(\tau)\lambda_\perp/R) v_y^S \\ &\times (\mathbf{x}^S(\tau))B(\tau) \equiv w_y^S(\mathbf{x}^S(\tau), \tau) \end{aligned} \tag{38}$$

with the initial condition

$$\mathbf{x}^S(0) = \mathbf{0} \tag{39}$$

$w_x^S(\mathbf{x}^S(\tau), \tau)$ and $w_y^S(\mathbf{x}^S(\tau), \tau)$ are the total velocities in a subensemble. In deriving system (37)–(38), we have made the assumption (specific to the DCT) that $\langle x(\tau)\rangle^S \simeq x^S(\tau)$. Using this assumption the following approximations are valid: $\langle x(\tau)K_{zs}^{\rm ion}\rangle^S \simeq x^S(\tau)K_{zs}^{\rm ion}$ and $\langle b^{-1}(x(\tau)\lambda_\perp/R)K^{\rm ion}\rangle^S \simeq (b^{-1}(x^S(\tau)\lambda_\perp/R))K^{\rm ion}$. The deterministic DCT solution of the system is used to obtain the approximate expression of the Lagrangian correlation (32), (33) where, instead of the

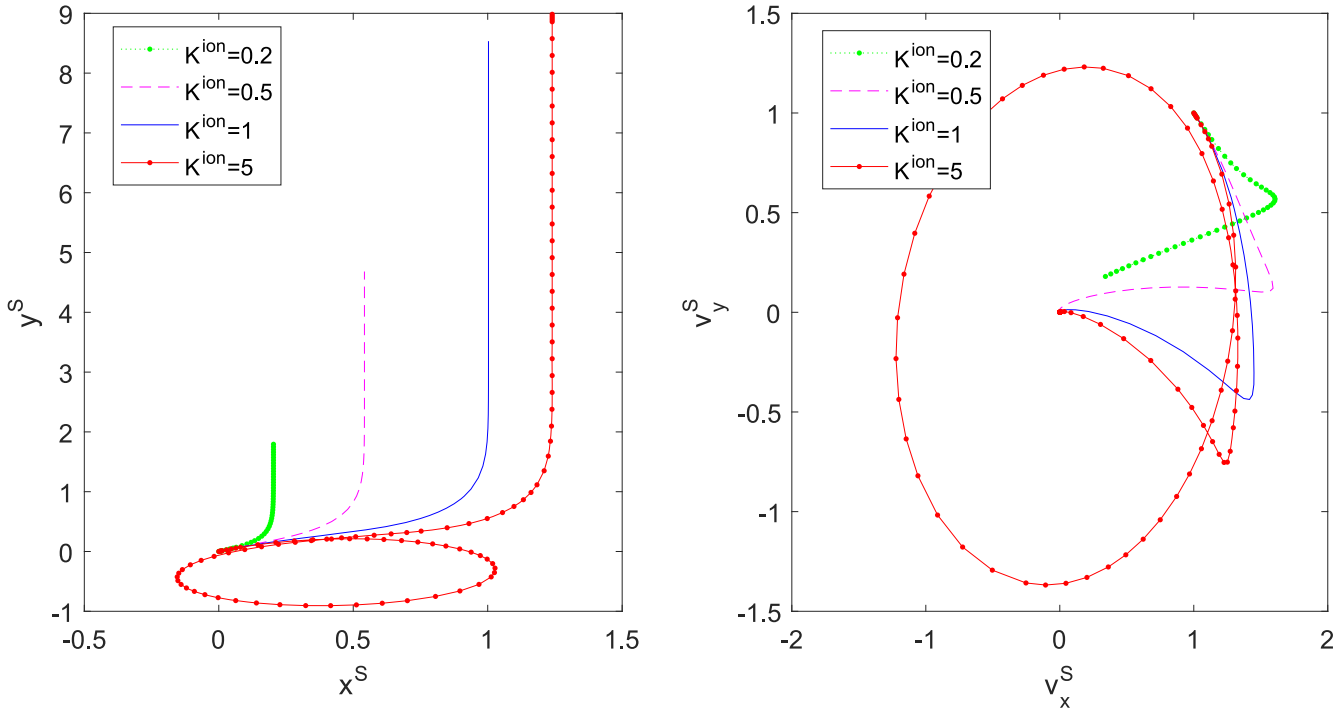

Figure 2. Trajectories and hodographs for $K_s^{\rm ion} = 1$, and four values of the level of turbulence in the subensemble given by $\varphi^0 = 2$, $v_x^0 = 1$ and $v_y^0 = 1$.

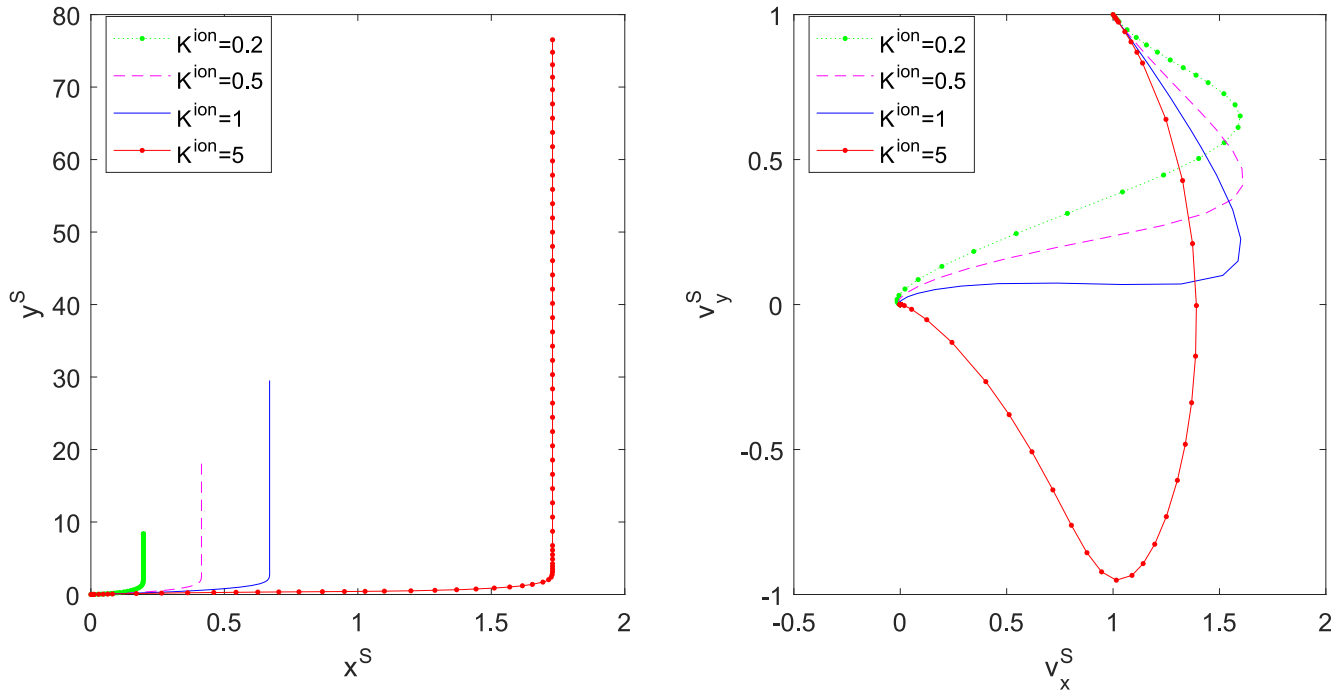

Figure 3. Trajectories and hodographs for $K_s^{\rm ion} = 5$, and four values of the level of turbulence in the subensemble given by $\varphi^0 = 2$, $v_x^0 = 1$ and $v_y^0 = 1$.

Lagrangian average of the velocity, the Eulerian average of the velocity calculated along the solution of system (37), (38) is used. The average in the subensemble S for the product of a deterministic function $F(x\lambda_\perp/R)$ and a directly fluctuating function, say $v_i(x, y, \tau; K_z^{\rm ion})$ $(i = x, y)$ will be calculated as

$$\langle F(x\lambda_\perp/R)v_i(x, y, \tau; K_z^{\rm ion})\rangle^S = F(x^S\lambda_\perp/R)\langle v_i(x, y, \tau; K_z^{\rm ion})\rangle^S \quad (40)$$

where the average $\langle v_i(x, y, \tau; K_z^{\rm ion})\rangle^S$ is performed using the DCT tools. In our case we need for the subensemble averaged

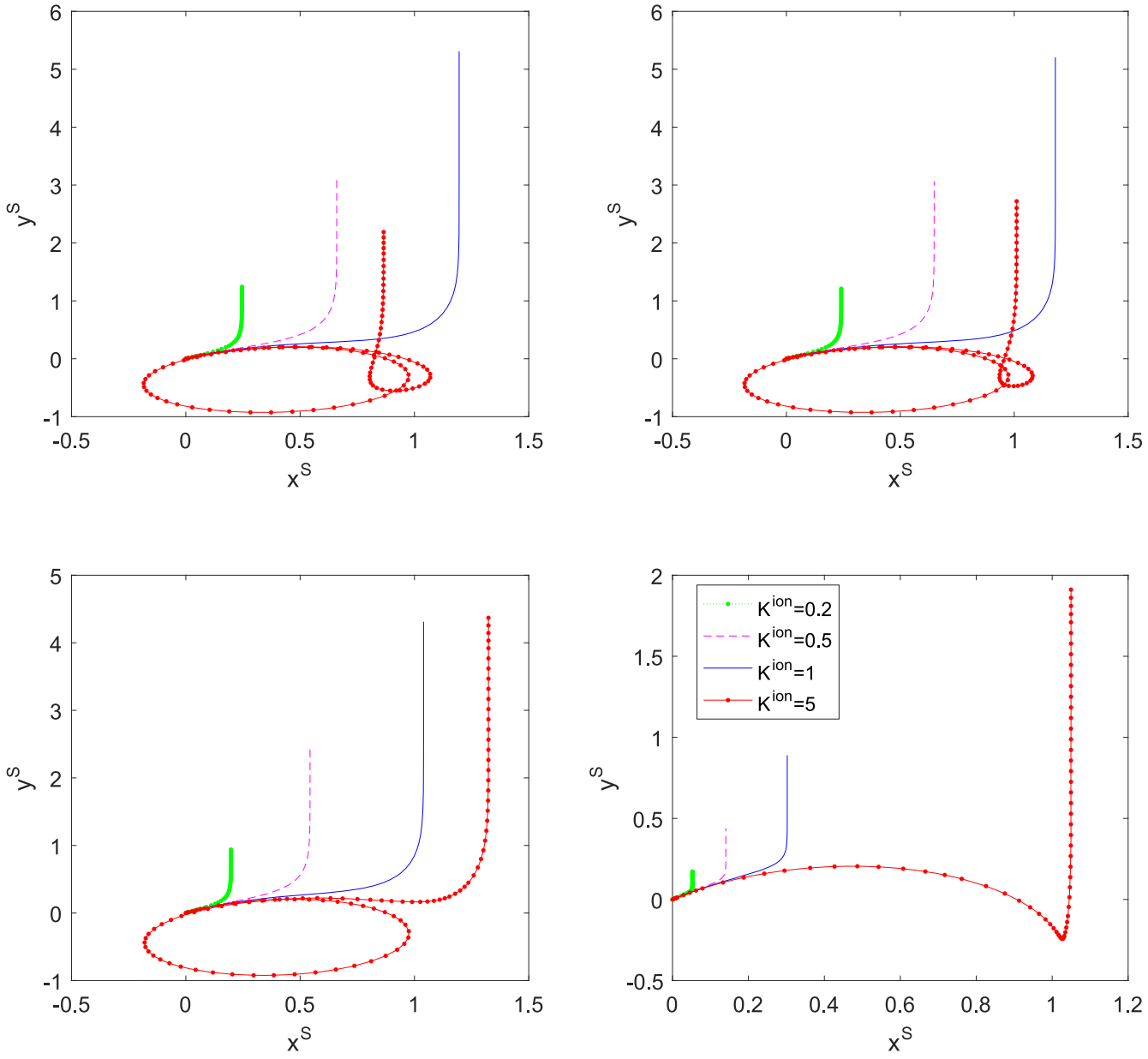

Figure 4. Trajectories in the subensemble given by $\varphi^0 = 2$, $v_x^0 = 1$ and $v_y^0 = 1$. In all subplots $K_s^{\rm ion} = 0.5$ and $K_z^{\rm ion} = 10^{-3}$ (top left), 10^{-2} (top right), 10^{-1} (bottom left), 1 (bottom right). Different values for the electrostatic Kubo number were used.

expressions of the following terms

$$K^{\rm ion} b^{-1}(x\lambda_\perp/R)\frac{\partial\varphi(x,\,y,\,\tau;\,K_z^{\rm ion})}{\partial y} = -K^{\rm ion} b^{-1}(x\lambda_\perp/R)v_x(x,\,y,\,\tau;\,K_z^{\rm ion}) \tag{41}$$

and

$$K^{\rm ion} b^{-1}(x\lambda_\perp/R)\frac{\partial\varphi(x,\,y,\,\tau;\,K_z^{\rm ion})}{\partial x} = K^{\rm ion} b^{-1}(x\lambda_\perp/R)v_y(x,\,y,\,\tau;\,K_z^{\rm ion}). \tag{42}$$

Using the equations (34), (35), (36), (40), (41) and (42) the terms are calculated as

$$b^{-1}(x^S\lambda_\perp/R)\langle v_x(x,\,y,\,\tau;\,K_z^{\rm ion})\rangle^S \equiv \equiv b^{-1}(x^S\lambda_\perp/R)[v_x^0(1-y^{2\,S})+v_y^0 x^S y^S+\varphi^0 y^S]C(\mathbf{x}^S,\,\tau) \tag{43}$$

and

$$b^{-1}(x^S\lambda_\perp/R)\langle v_y(x,\,y,\,\tau;\,K_z^{\rm ion})\rangle^S \equiv \equiv b^{-1}(x^S\lambda_\perp/R)[v_x^0 x^S y^S+v_y^0(1-x^{2\,S})-\varphi^0 x^S]C(\mathbf{x}^S,\,\tau). \tag{44}$$

The solution of deterministic system (37), (38) depends not only on the parameters that define the subensemble S i.e. $[\varphi(\mathbf{0},\,0)=\varphi^0,\,\mathbf{v}(\mathbf{0},\,0)=\mathbf{v}^0]$ but also on the Kubo numbers defined in equations (7), (8), (10).

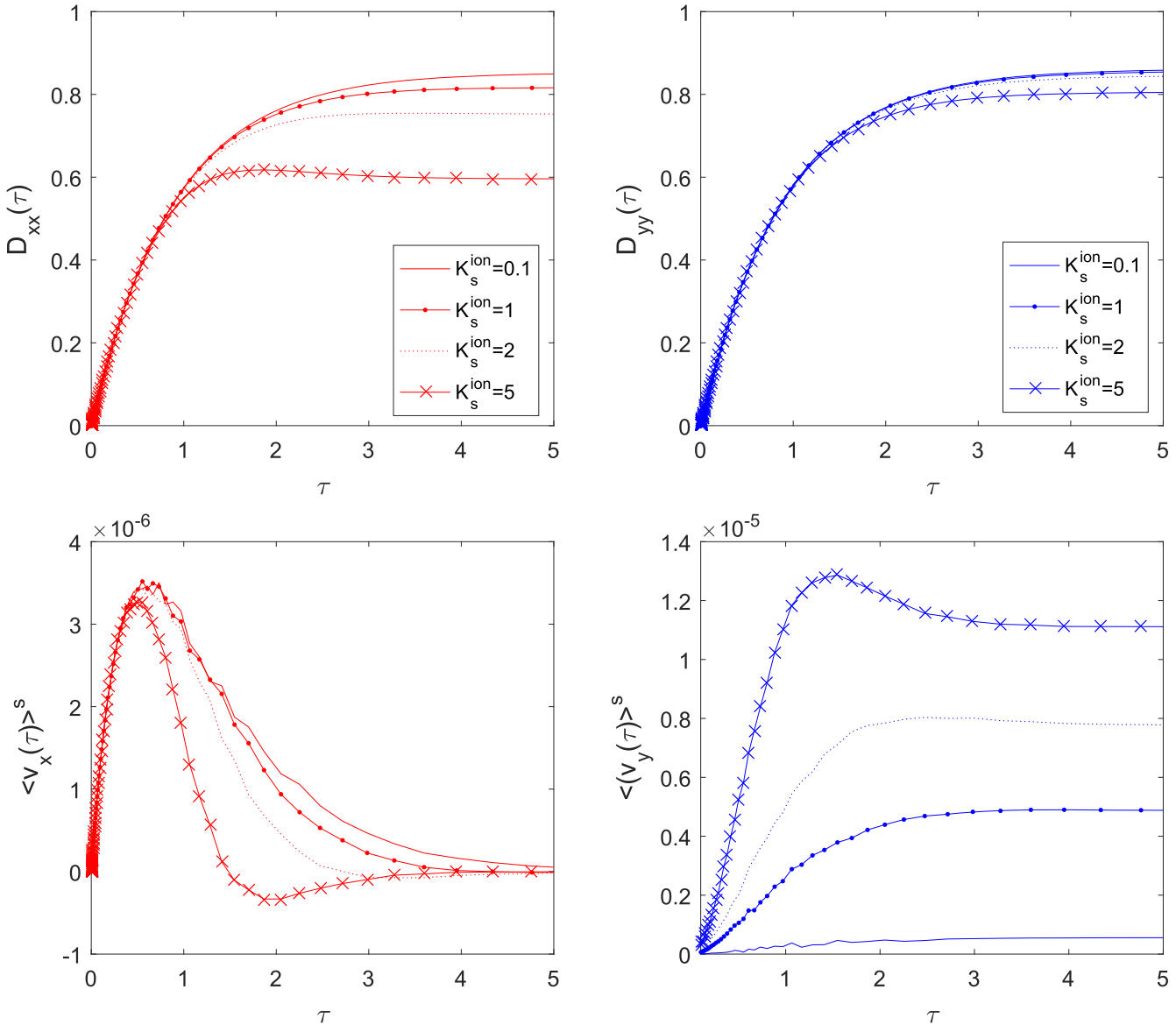

Figure 5. Diffusion coefficients and averaged velocities for $K^{\rm ion} = 0.2$ and $K_{\rm s}^{\rm ion} \in \{0.1, 1, 2, 5\}$.

The Lagrangian correlation tensor components are

$$L_{ij}(\tau) = (2\pi)^{-\frac{3}{2}} \int \mathrm{d}\varphi^0 \int \mathrm{d}v_x^0 \int \mathrm{d}v_y^0 \exp\left\{-\frac{1}{2}[(v_x^0)^2 + (v_y^0)^2 + (\varphi^0)^2]\right\} L_{ij}^S(\tau) \tag{45}$$

and contribute to the calculation of the running diffusion tensor components as

$$D_{ij}(\tau) = \int_0^\tau L_{ij}(\theta)\mathrm{d}\theta. \tag{46}$$

For $K_{\rm z}^{\rm ion} \ll 1$, i.e. $\frac{K}{K_{\rm z}^{\rm ion}+1} \simeq K$ the diffusion coefficient is influenced directly only by K^2 and implicitly by $K_{\rm s}^{\rm ion}$. For $K_{\rm z}^{\rm ion} \simeq 1$ the diffusion coefficient is influenced directly by $\left(\frac{K}{K_{\rm z}^{\rm ion}+1}\right)^2$ and implicitly by $K_{\rm zs}^{\rm ion}$.

4. DCT trajectories

In this section we present some trajectories and hodographs resulting from system (37), (38), for a subensemble defined as S: $\varphi(\mathbf{0}, 0) = \varphi^0 = 2$, $v_x(\mathbf{0}, 0) = v_x^0 = 1$ and $v_y(\mathbf{0}, 0) = v_y^0 = 1$ and for different values of $K^{\rm ion}$ and $K_{\rm s}^{\rm ion}$ ($K_{\rm z}^{\rm ion} \ll 1$). In figures 1–3 we visualized trajectories and hodographs for the set of electrostatic Kubo numbers [0.2, 0.5, 1, 5] for different values of the shear Kubo number $K_{\rm s}^{\rm ion} = 0.5$ (figure 1), $K_{\rm s}^{\rm ion} = 1$ (figure 2) and $K_{\rm s}^{\rm ion} = 5$ (figure 3). The shape is influenced by the electrostatic Kubo number only for a relatively high value of the level of turbulence as shown in the figures. For relatively small values [$K^{\rm ion} = 0.5$, 1] of the level of turbulence, the shapes are almost the same except for the high value [$K^{\rm ion} = 5$] (see figures 1–3).

All these quantities are calculated for different values of the electrostatic Kubo number $K^{\rm ion} \equiv \frac{K}{K_{\rm z}^{\rm ion}+1}$ defined above

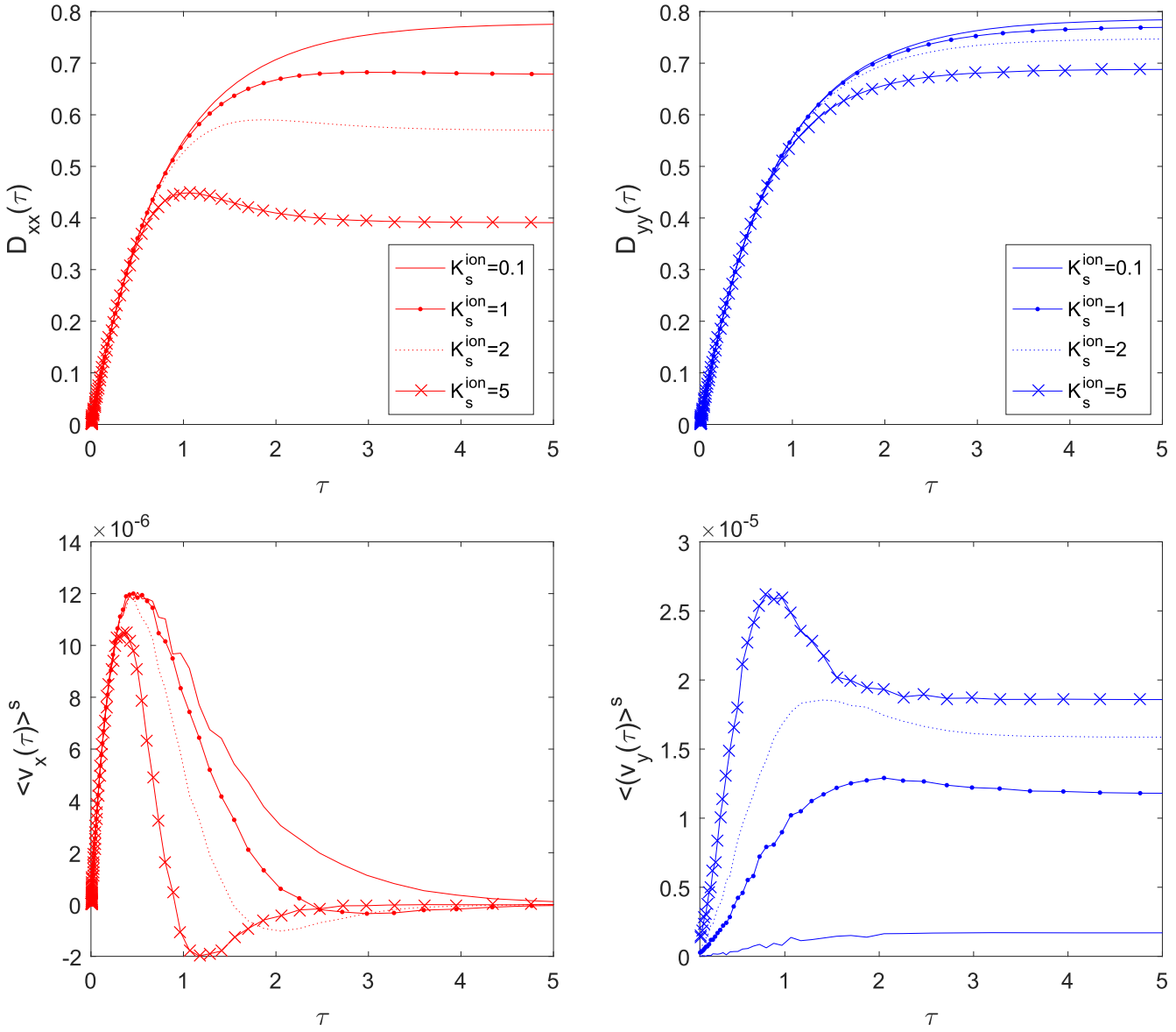

Figure 6. Diffusion coefficients and averaged velocities for $K^{\rm ion} = 0.5$ and $K_{\rm s}^{\rm ion} \in \{0.1, 1, 2, 5\}$.

in expression (28) and of the shear Kubo number $K_{\rm zs}^{\rm ion} \equiv \frac{K_{\rm s}^{\rm ion}}{K_{\rm z}^{\rm ion}+1}$ defined in expression (29); the aforementioned Kubo numbers depend on $K_{\rm z}^{\rm ion} = \frac{V_{\rm th}^{\rm ion}\tau_{\rm c}}{\lambda_{\parallel}} \in [10^{-2}, 1]$. The value $K_{\rm z}^{\rm ion} = 10^{-3}$ was used in order to investigate the influence of this order of magnitude on the trajectory shape: this is not important as we can see from figure 4.

We have used in our calculations the electrostatic Kubo numbers

$$K^{\rm ion} \in \{0.2, 1, 5, 10\}.$$

For each value of the electrostatic Kubo number we have considered the evolution of the quantities for different values of the shear Kubo numbers

$$K_{\rm s}^{\rm ion} \in \{0.1, 1, 2, 5\}.$$

Figure 4 presents the trajectories for a given subensemble, four fixed values for the electrostatic Kubo number $K^{\rm ion}$, a fixed value of the shear Kubo number $K_{\rm s}^{\rm ion} = 0.5$ and different values of the parameter $K_{\rm z}^{\rm ion}$: in the top left subplot $K_{\rm z}^{\rm ion} = 10^{-3}$, in the top right subplot $K_{\rm z}^{\rm ion} = 10^{-2}$, in the bottom left subplot $K_{\rm z}^{\rm ion} = 10^{-1}$ and in the bottom right subplot $K_{\rm z}^{\rm ion} = 1$. The trajectories are closed for $K^{\rm ion} = 5$ and open in all the other cases, i.e. 0.2, 0.5, and 1 if $K_{\rm z}^{\rm ion} < 1$. For $K_{\rm z}^{\rm ion} = 1$ the trajectories corresponding to $K^{\rm ion} = 5$ are also open, so trapping is not present in this case.

4.1. Comments on Kubo numbers and trapping versus open trajectories

In the subensemble defined as S: $\varphi(\mathbf{0}, 0) = \varphi^0 = 2$, $v_x(\mathbf{0}, 0) = v_x^0 = 1$ and $v_y(\mathbf{0}, 0) = v_y^0 = 1$ the shapes of the trajectories represented in figures 1–4 are influenced by the parameters already mentioned before.

Trapping (or the existence of closed trajectories) is present when particles are moving near the maxima or minima of

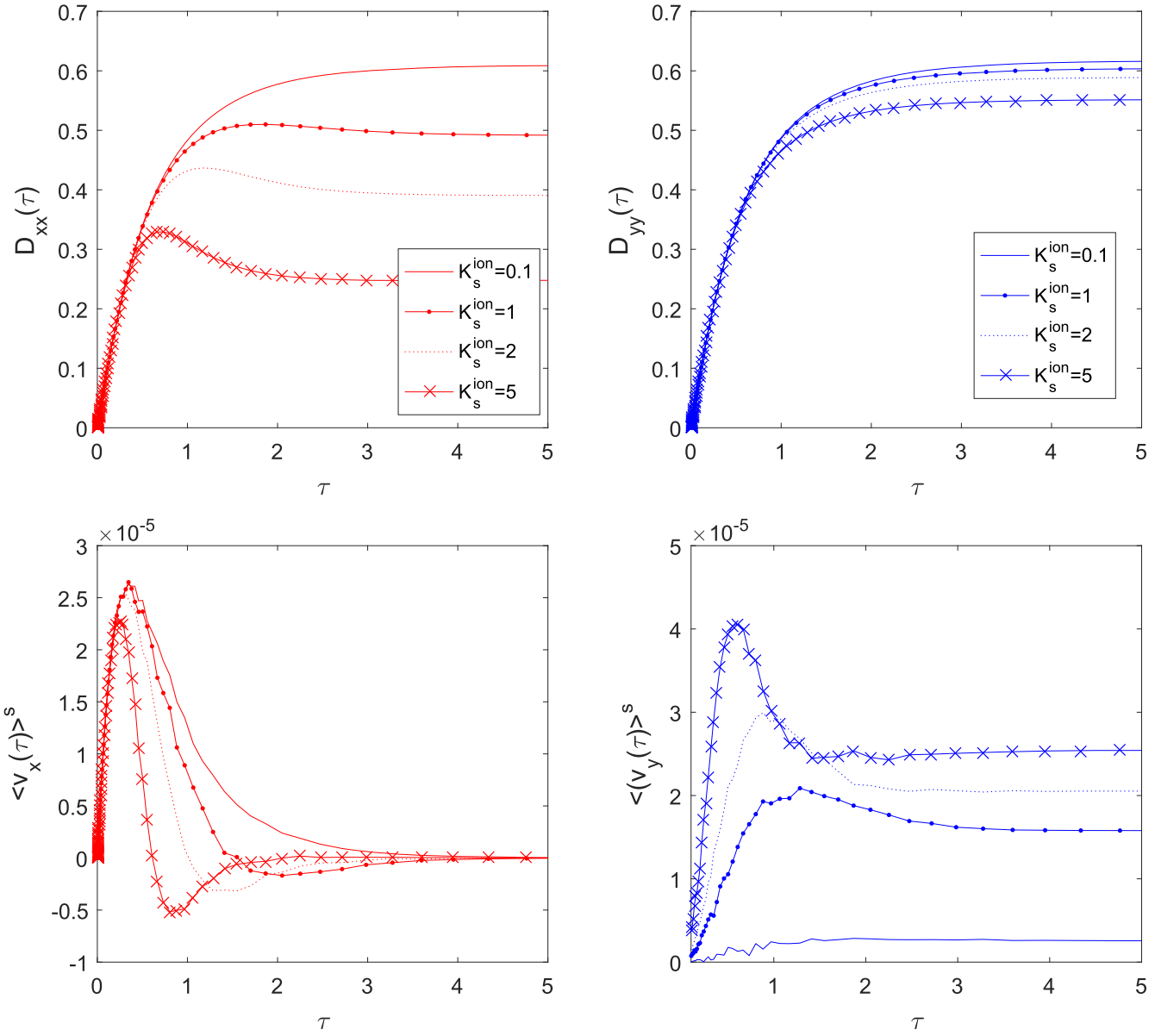

Figure 7. Diffusion coefficients and averaged velocities for $K^{\text{ion}} = 1$ and $K_{\text{s}}^{\text{ion}} \in \{0.1, 1, 2, 5\}$.

the stochastic electrostatic potential, and is influenced by dimensionless quantities called Kubo numbers. In our paper there are several Kubo numbers defined in (7)–(10), (12) and (13) in the particular case of ions. The electrostatic Kubo number defined in (7) measures the stochastic character of the electrostatic field and represents the ratio between the distance $V_{\text{th}}\tau_{\text{c}}$ covered by a particle moving with the velocity V_{th} during the correlation time τ_{c} and the perpendicular correlation length $\lambda_\perp$,

$$K = \frac{V_{\text{th}}\tau_{\text{c}}}{\lambda_\perp} \equiv \frac{\varepsilon\tau_{\text{c}}}{B_0\lambda_\perp^2} \equiv \frac{\tau_{\text{c}}}{\tau_{\text{fl}}}$$

where $\tau_{\text{fl}} = \left(\frac{V_{\text{th}}}{\lambda_\perp}\right)^{-1}$ is the time of flight, i.e. the time necessary for the particle to cover a distance of the order of magnitude of the correlation length. Similar definitions for Kubo numbers are given in expressions (8) (where in K_{s} the interchange $\lambda_\perp \Longleftrightarrow L_{\text{s}}$ is obvious) and (10) (where in K_{z} the interchange $\lambda_\perp \Longleftrightarrow \lambda_\parallel$ is made). In (9) where K_{zs} is defined, the interchange $\lambda_\perp^2 \Longleftrightarrow L_{\text{s}}\lambda_\parallel$ is made. In figure 4 the influence of $K_{\text{z}}^{\text{ion}}$ on the shape of trajectories is featured. The trajectories are closed (trapping) only for $K^{\text{ion}} = 5$. Two closures are observed for $K^{\text{ion}} = 5$, $K_{\text{s}}^{\text{ion}} = 0.5$ and for two values $K_{\text{z}}^{\text{ion}} = 10^{-3}$ and 10^{-2}. If $K_{\text{z}}^{\text{ion}}$ increases the trajectories become open (see the case where $K_{\text{z}}^{\text{ion}} = 1$). For a fixed parallel correlation length, the variation of the thermal velocity modifies the parallel time of flight $\tau_{\text{fl}}^{\parallel} = \left(\frac{V_{\text{th}}}{\lambda_\parallel}\right)^{-1}$: the greater the thermal velocity, the shorter the time of flight is and the fewer open trajectories are present.

5. Diffusion coefficients

In this section we present in figures 5–9 the behavior of the running poloidal and radial diffusion coefficients (D_{yy}, D_{xx})

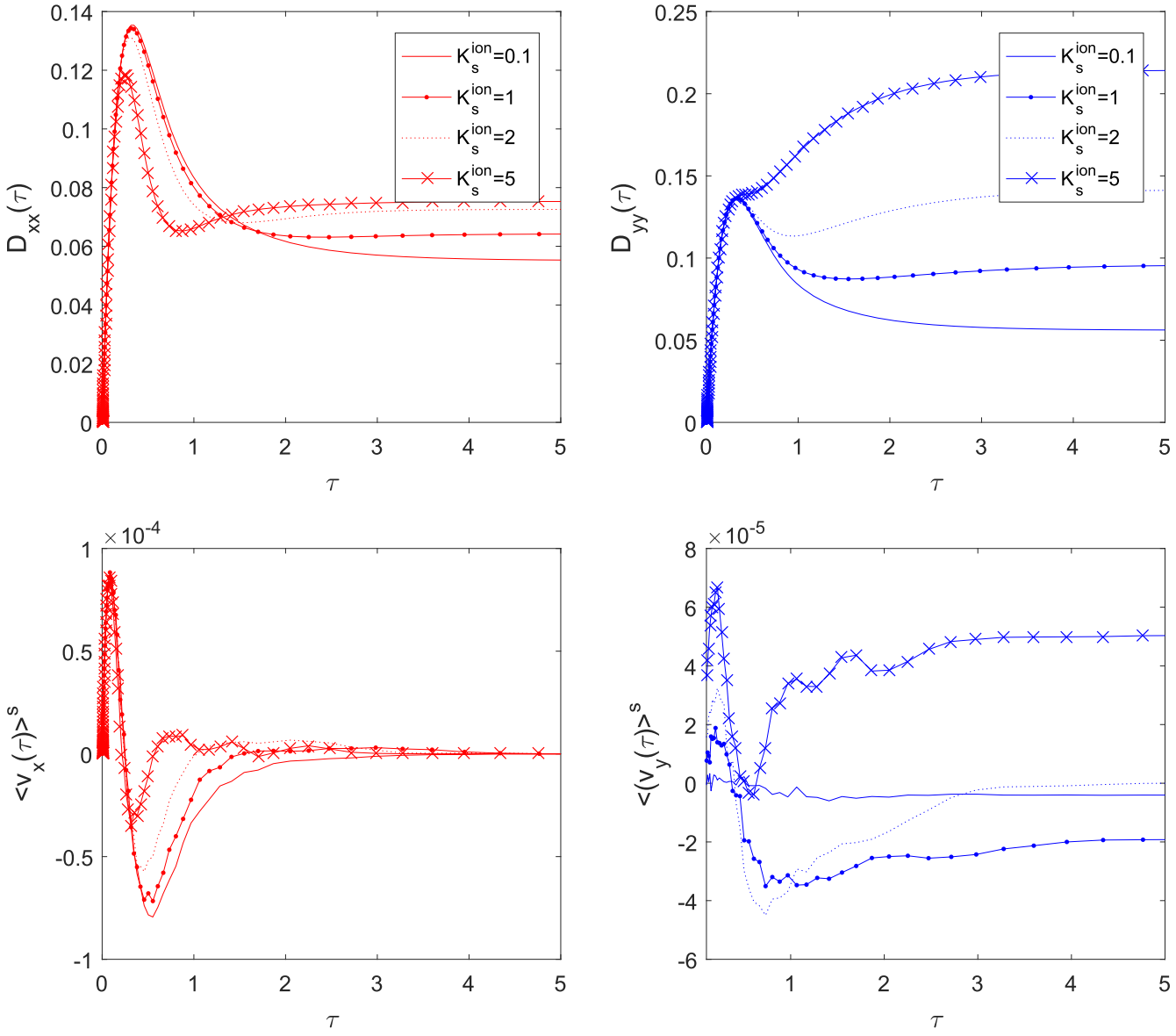

Figure 8. Diffusion coefficients and averaged velocities for $K^{ion} = 5$ and $K_s^{ion} \in \{0.1, 1, 2, 5\}$.

and the averaged directly fluctuating velocities over the sub-ensembles, i.e. $\langle v_k(\mathbf{x}^S(\tau), \tau)\rangle^S$, $k = x, y$. In figures 5–9 the following labels are used for the radial running diffusion coefficients: $K_s^{ion} = 0.1$ (continuous red line), $K_s^{ion} = 1$ (continuous dotted red line), $K_s^{ion} = 2$ (dotted red line) and $K_s^{ion} = 5$ (continuous red x line) and the same labels in blue for the poloidal running diffusion coefficients. For $K^{ion} = 0.2$ the smallest asymptotic value (≈0.6) of the radial diffusion coefficient D_{xx} is obtained for the greater value of the shear Kubo number, i.e. $K_s^{ion} = 5$; the same behavior is obtained for the poloidal diffusion coefficient D_{yy} but the asymptotic value is different (≈0.75) (see figure 5). The averaged directly fluctuating velocities $\langle v_k(\mathbf{x}^S(\tau), \tau)\rangle^S$ are represented also in figure 5; the poloidal one is positive for $\forall \tau \geqslant 0$ but the radial one is negative for $K_s^{ion} = 5$ and positive for the other values of K_s^{ion} for the entire time interval $\tau \in [0, 4]$. The asymptotic (i.e. for $\tau \geqslant 4$) values of the averaged velocities are all zero. Practically the same behavior is present for $K^{ion} = 0.5$ but with other values for the asymptotic diffusion coefficients (see figure 6). For $K^{ion} = 1$, the smallest asymptotic value (≈0.25) for the radial diffusion coefficient D_{xx} is obtained for the greater value of the shear Kubo number, i.e. $K_s^{ion} = 5$; the same behavior is obtained for the poloidal diffusion coefficient D_{yy} but the asymptotic value is different (≈0.5) (see figure 7).

The averaged directly fluctuating velocities $\langle v_k(\mathbf{x}^S(\tau), \tau)\rangle^S$ also represented in figure 7 are positives for $\forall \tau \geqslant 0$ except for the radial one, which is negative for $K_s^{ion} = 5$ in the interval $\tau \in [1, 2]$. The asymptotic values are all zero.

For $K^{ion} = 5$ the asymptotic radial diffusion coefficient values are diminished and they belong to the interval [0.06, 0.075], but the small one is obtained for $K_s^{ion} = 0.1$ (see figure 8). For an increased value of the electrostatic Kubo number ($K^{ion} = 10$) an inversion of the behavior of the

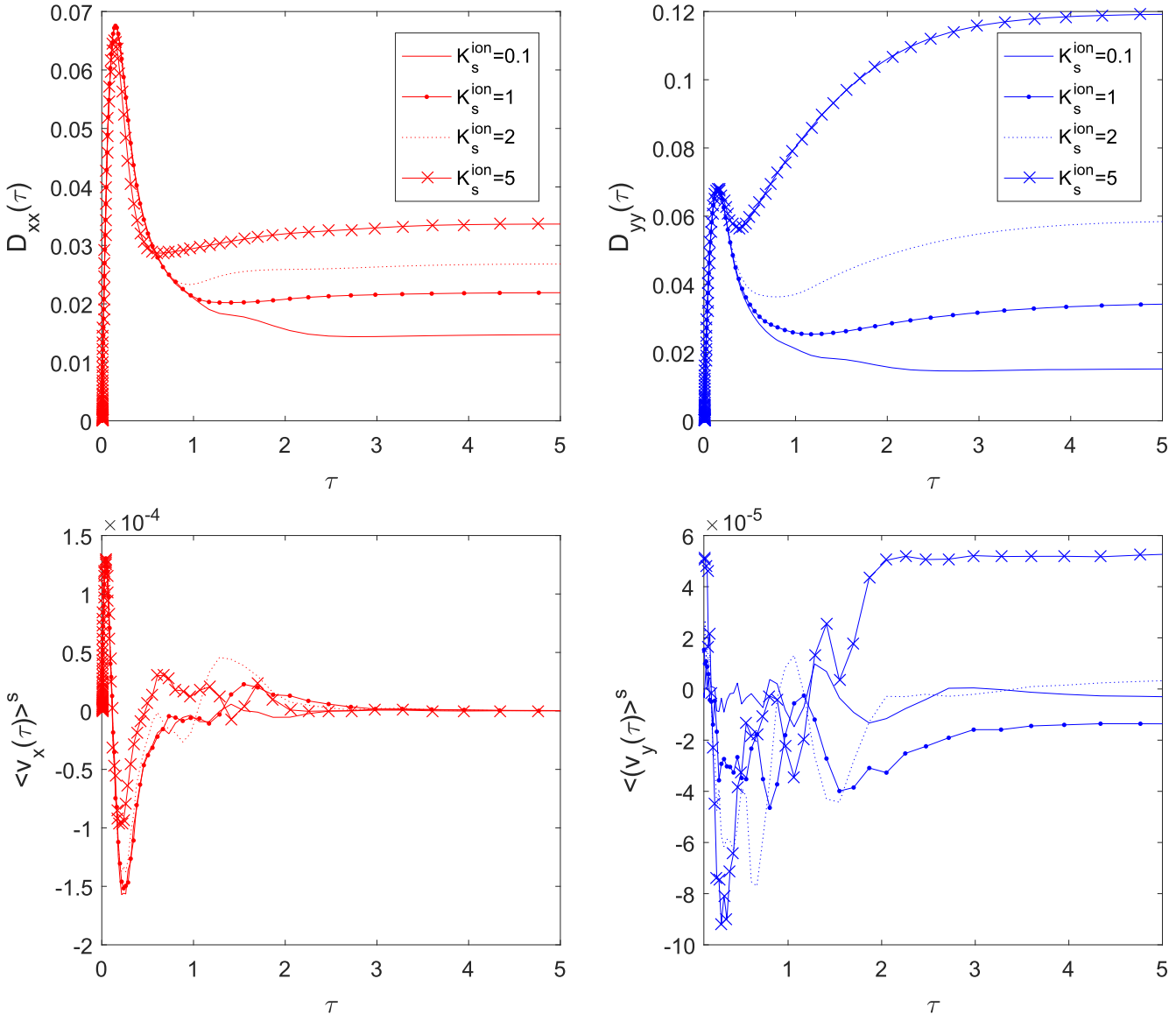

Figure 9. Diffusion coefficients and averaged velocities for $K^{\text{ion}} = 10$ and $K_{\text{s}}^{\text{ion}} \in \{0.1, 1, 2, 5\}$.

diffusion coefficients is observed (see figure 9); a decreasing of the maximum of the radial diffusion coefficient is also observed. The dimensional expressions for the radial and poloidal diffusion coefficients are

$$D_{XX} = D_{xx}\frac{V_{\text{th}}\lambda_{\perp}^2}{\lambda_{\parallel}} = cD_{xx} \tag{47}$$

and

$$D_{YY} = D_{yy}\frac{V_{\text{th}}\lambda_{\perp}^2}{\lambda_{\parallel}} = cD_{yy} \tag{48}$$

respectively. If we consider $\lambda_{\parallel} \simeq 1$ m, $\lambda_{\perp} \simeq 10^{-2}$ m and $V_{\text{th}} \simeq 10^5\,\text{m}\,\text{s}^{-1}$ the dimensional factor c is about

$$c = 10\ \text{m}^2\,\text{s}^{-1}.$$

The expressions of D_{XX} and D_{YY} can be defined also as functions of $K_{\text{z}}^{\text{ion}} = \frac{V_{\text{th}}^{\text{ion}}\tau_{\text{c}}}{\lambda_{\parallel}}$ as

$$D_{XX} = D_{xx}\frac{V_{\text{th}}\lambda_{\perp}^2}{\lambda_{\parallel}} \equiv K_{\text{z}}^{\text{ion}}(\tau_{\text{c}})^{-1}D_{xx}\lambda_{\perp}^2 \tag{49}$$

and

$$D_{YY} = D_{yy}\frac{V_{\text{th}}\lambda_{\perp}^2}{\lambda_{\parallel}} \equiv K_{\text{z}}^{\text{ion}}(\tau_{\text{c}})^{-1}D_{yy}\lambda_{\perp}^2 \tag{50}$$

where we remember that the correlation time is about $\tau_{\text{c}} \simeq 10^{-5}$ s. As a consequence,

$$D_{XX} = D_{xx}\frac{V_{\text{th}}\lambda_{\perp}^2}{\lambda_{\parallel}} \equiv K_{\text{z}}^{\text{ion}}(\tau_{\text{c}})^{-1}D_{xx}\lambda_{\perp}^2 = 10\ K_{\text{z}}^{\text{ion}}D_{xx}$$
$$D_{YY} = D_{yy}\frac{V_{\text{th}}\lambda_{\perp}^2}{\lambda_{\parallel}} \equiv K_{\text{z}}^{\text{ion}}(\tau_{\text{c}})^{-1}D_{yy}\lambda_{\perp}^2 = 10\ K_{\text{z}}^{\text{ion}}D_{yy}. \tag{51}$$

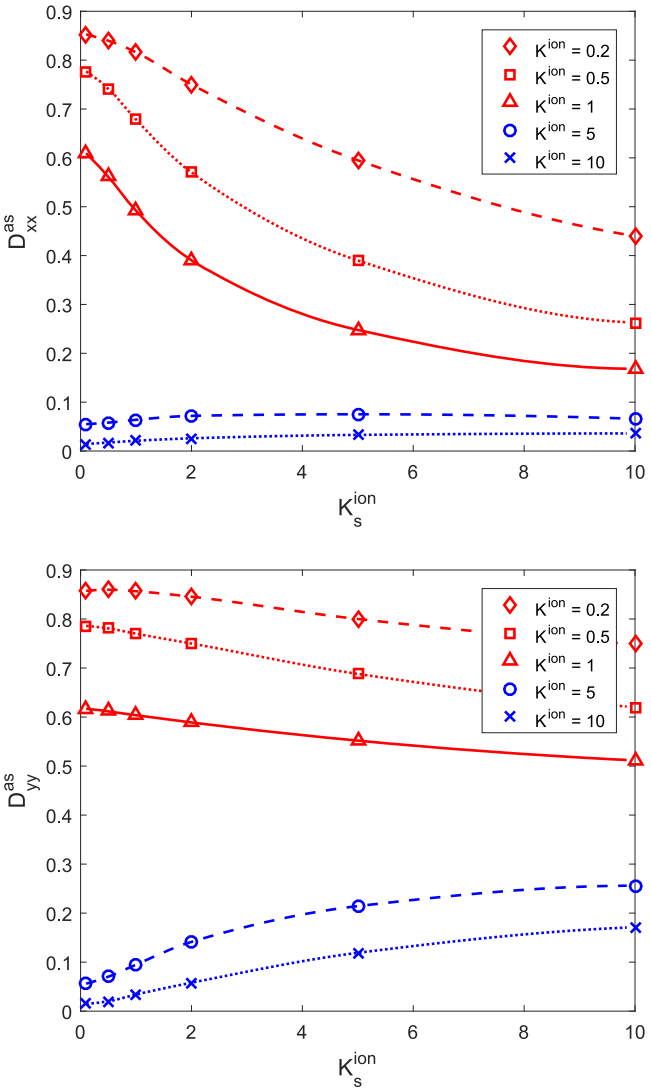

Figure 10. Radial and poloidal asymptotic diffusion coefficients as a function of K_s^{ion} for different values of the level of electrostatic turbulence given by K^{ion}.

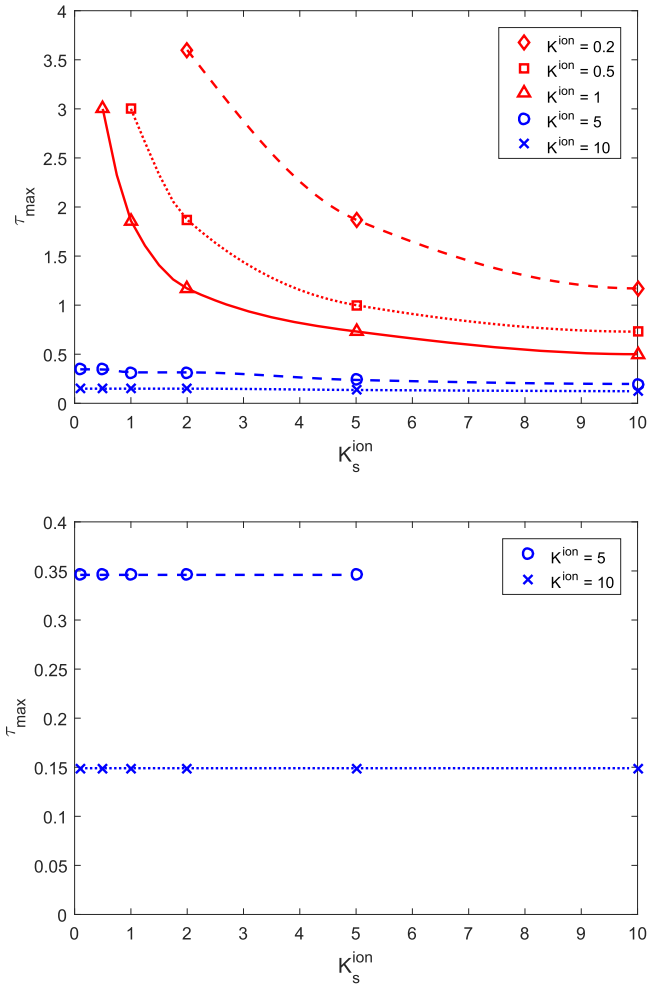

Figure 11. The moments corresponding to the achievements of maxima for the radial and poloidal diffusion coefficients as a function of K_s^{ion} for different values of K^{ion}.

In conclusion, varying K_z^{ion} we obtain the corresponding maxima and minima for D_{ii} $(i = X, Y)$

$$(D_{XX})^{max} = 10\ D_{xx},\quad K_z^{ion} = 1$$
$$(D_{YY})^{max} = 10\ D_{yy},\quad K_z^{ion} = 1 \qquad (52)$$

and

$$(D_{XX})^{min} = 10^{-1}\ D_{xx},\quad K_z^{ion} = 10^{-2}$$
$$(D_{YY})^{min} = 10^{-1}\ D_{yy},\quad K_z^{ion} = 10^{-2}. \qquad (53)$$

Using the above relations and the results shown in the corresponding figures, we can state some observations. As stated in [33] for example, the neoclassical values for the diffusion coefficients are smaller than unity; e.g. they are of the order of 0.5 $m^2\ s^{-1}$, whereas in experiments they are much larger, with anomalous values that are found to be of the order of 4 $m^2\ s^{-1}$.

For $K^{ion} = 10$ (see figure 9) the radial diffusion coefficient $(D_{XX})^{max}$ is in the range of the neoclassical values, i.e. $(D_{XX})^{max} \simeq 0.7\ m^2\ s^{-1}$ for practically all values of K_s^{ion}. The same situation appears for $(D_{YY})^{max} \simeq 0.6\ m^2\ s^{-1}$ for practically all values of K_s^{ion}. For the asymptotic values of the radial diffusion coefficients the situation is the following: $(D_{XX})^{as}$ is in the range [0.15, 0.35], and increases if K_s^{ion} increases to the range [0.1, 5]. $(D_{XX})^{as}$ is about 0.6 $m^2\ s^{-1}$ practically for all K_s^{ion}. $(D_{YY})^{as}$ is in the range [0.2, 1.2] and increases if K_s^{ion} increases to the range [0.1, 5].

For $K^{ion} = 5$ (see figure 8), $K_s^{ion} = 0.1$ and 1, the radial diffusion coefficient has the maxima values $(D_{XX})^{max} \simeq 1.4\ m^2\ s^{-1}$ for $K_z^{ion} = 1$ and 0.014 for $K_z^{ion} = 10^{-2}$. $(D_{YY})^{as}$ is in the range [0.75, 2] and increases if K_s^{ion} increases to the range [0.1, 5]. In figures 10–12 the labels used are as follows: $K^{ion} = 0.2$ (red diamond), $K^{ion} = 0.5$ (red squared), $K^{ion} = 1$ (red triangle), $K^{ion} = 5$ (blue circle) and $K^{ion} = 10$ (blue x). We have calculated the influence of K_s^{ion} on the radial and poloidal asymptotic diffusion coefficients for different levels of the electrostatic turbulence (see figure 10). It is obvious that an increase of the shear Kubo number produces a

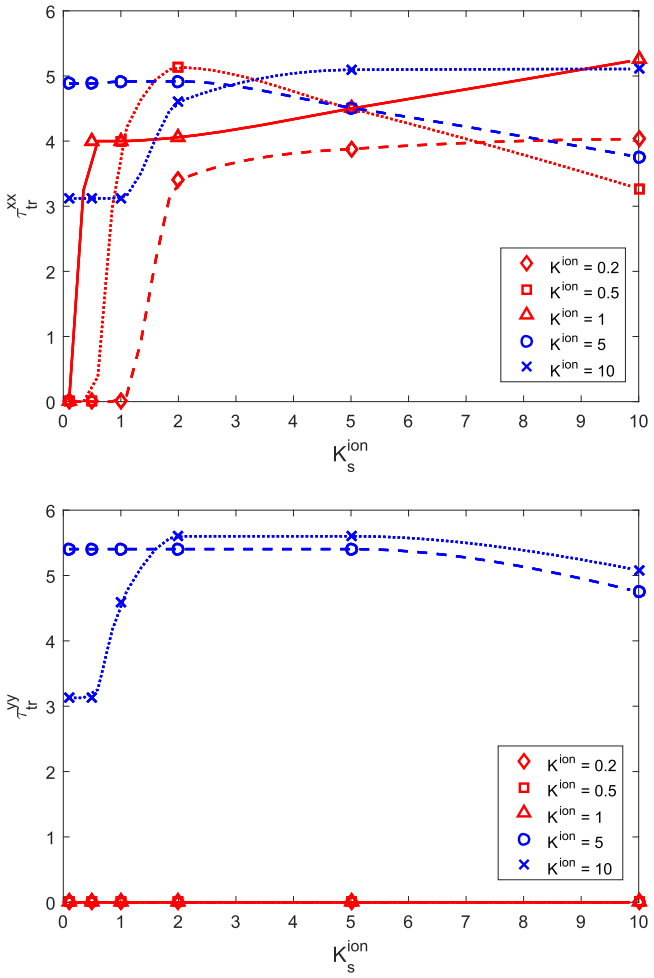

Figure 12. Radial and poloidal trapping time as a function of K_s^{ion} for different values of the level of electrostatic turbulence given by K^{ion}.

decrease of the asymptotic values for the radial and poloidal diffusion coefficients except for the level of electrostatic turbulence given here by $K^{ion} = 5$, $K^{ion} = 10$; the asymptotic values increase slowly as a function of K_s^{ion} but the final values are smaller than those corresponding to $K^{ion} < 5$. In figure 11 the moments τ_{max} corresponding to the maxima achievements are represented as a function of K_s^{ion} for different K^{ion}. For the radial diffusion coefficients (top of figure 11) the shapes are very similar to a hyperbolic decrease as a function of K_s^{ion}. The following order is obvious

$$(\tau_{max})_{0.2} > (\tau_{max})_{0.5} > (\tau_{max})_1 > (\tau_{max})_5 > (\tau_{max})_{10}. \quad (54)$$

The smallest value is $(\tau_{max})_{10}$ and corresponds to $K^{ion} = 10$. For the poloidal diffusion we represented in (bottom of figure 11) τ_{max} only for $K^{ion} = 5$, $K^{ion} = 10$. There are constant values for these moments; only their order of magnitude is different. We have also calculated the influence of K_s^{ion} on the trapping time interval, i.e. on $\tau_{tr} = \tau_{as} - \tau_{max}$, where τ_{as} is the moment corresponding to the beginning of the asymptotic regime and τ_{max} is the moment that corresponds to the maxima of the diffusion coefficients (see figure 12). We note that if trapping is present the diffusion coefficient shape begins with an increase (the ballistic regime) and continues with a subdiffusion regime up to a value corresponding to the beginning of the asymptotic regime. For the radial diffusion coefficient, we conclude that the trapping time τ_{tr}^{xx} increases for $K_s^{ion} \leqslant 2$ for $K^{ion} \in \{0.2, 0.5, 1\}$ and has relatively constant values for $K^{ion} \in \{5, 10\}$ also for $K_s^{ion} \leqslant 2$. For $K_s^{ion} \geqslant 2$ a relatively small region with a decrease of the time trapping is present for $K^{ion} = 5$ followed by a decrease and an increase followed by a constant regime for $K^{ion} = 10$. For $K^{ion} = 0.2$ and 1 there exists a small increase, and for $K^{ion} = 0.5$ a decrease is present. For the poloidal diffusion coefficient the shape of the trapping time τ_{tr}^{yy} represented in figure 12 only for a relatively large turbulence level is practically the same as for the corresponding radial situation.

6. Conclusions

In this paper, we have analyzed the diffusion of the ions using the Langevin equations corresponding to the guiding center and we applied the semi-analytical method of decorrelation trajectories (DCT). The latter can be considered as a generalization of the Corrsin approximation and takes into account the trapping effects (which necessarily exist in relatively strong turbulent plasmas). Using DCT, we have studied the transport of test particles (ions) by the electromagnetic drift that is produced by a stochastic electrostatic potential and by an inhomogeneous and sheared magnetic field. The DCT and the model used have given good qualitative results concerning the diffusion of ions. The radial and poloidal coefficients start with a linear part, indicating a ballistic regime, which is followed by a trapping regime. If trapping is present the diffusion coefficient has a shape that begins with an increase of the diffusion coefficient (the ballistic regime) and continues with a subdiffusion regime up to a value corresponding to the beginning of the asymptotic regime. We have calculated the influence of K_s^{ion} on the radial and poloidal trapping time intervals for different values of K^{ion}. After that the asymptotic value is reached (the trapping effects are visible in representations of trajectories). The diffusion coefficients increase with increasing levels of turbulence, i.e. with an increasing K^{ion}. We have also represented the dependence of τ_{max} as a function of K_s^{ion} and the trapping time interval as a function of K_s^{ion} for different levels of electrostatic turbulence. The maximum radial trapping time is reached for $K^{ion} = 0.5$ for $K_s^{ion} = 2$. The value $K_s^{ion} = 2$ represents a critical value to which a corresponding critical value for the thermal ion velocity is obtained. For fixed values of the shear length and of the correlation time this critical value can be obtained. For $L_s = 10$ m, $\tau_c = 10^{-5}$ s, the critical thermal velocity is $(V_{th})^{cr} = 2 \times 10^6$ m s^{-1}. The results obtained in our model are in agreement with the experimental data: the neoclassical and anomalous values for the diffusion coefficients are obtained. Here the magnetic field model dependence on the radial coordinate and the electrostatic stochastic field influenced the values of the diffusion coefficients. Concerning the diffusion coefficients, similar results with those obtained in the present paper were found in [30]. The conclusion is that from these two different physical

models we obtained practically the same diffusion coefficient behavior. The magnetic shear, the inhomogeneity of the magnetic field and also the stochastic electrostatic field have the same influence on the ions' diffusion as has the stochastic magnetic drift.

In conclusion, we state that

(a) the diffusion present a pronounced trapping if $K^{\text{ion}} \geqslant 5$;
(b) the maxima of the diffusion coefficients decreases if $K^{\text{ion}} \geqslant 5$;
(c) the space dependence and the shear of the magnetic field modifies the diffusion coefficients.

Important results concerning the behavior of the magnetic field were obtained (see e.g. [34] and [35]) analyzing the Grad–Shafranov equation. From here, the possibility of constructing different magnetic fields appears. The diffusion of stochastic isotropic and anisotropic magnetic field lines in turbulence with a magnetic average poloidal magnetic field component was studied in [36] and an extension of this paper in such a magnetic field would be of interest. It will be necessary that collisions are taken into consideration in such a study, but this issue is left for future work. Here, only the influence of the aforementioned parameters on motion were taken into account.

Acknowledgments

I would like to thank Dr. Iulian Petrisor for fruitful discussions. This work has been carried out within the framework of the EUROfusion Consortium and has received funding from the EURATOM research and training program 2014–2018 under Grant Agreement No. 633053. The views and opinions expressed herein do not necessarily reflect those of the European Commission.

ORCID iDs

Marian NEGREA https://orcid.org/0000-0002-5455-5031

References

[1] Balescu R 1988 *Transport Processes in Plasmas, vol I Classical Transport* (Amsterdam: North-Holland)
[2] Balescu R 1988 *Transport Processes in Plasmas, vol II, Neoclassical Transport* (Amsterdam: North-Holland)
[3] Hinton F L and Hazeltine R D 1976 *Rev. Mod. Phys.* **48** 239
[4] Isichenko M B 1991 *Plasma Phys. Contr. Fusion* **33** 795
[5] Isichenko M B 1992 *Rev. Mod. Phys.* **64** 961
[6] Ottaviani M 1992 *Europhys. Lett.* **20** 111
[7] Misguich J H *et al* 1998 *Physicalia Mag.* **20** 103
[8] Petrisor I 2016 *Rom. J. Phys.* **61** 217
[9] Vlad M *et al* 1998 *Phys. Rev.* E **58** 7359
[10] Vlad M *et al* 2002 *Nucl. Fusion* **42** 157
[11] Negrea M, Petrisor I and Balescu R 2004 *Phys. Rev.* E **70** 046409
[12] Balescu R, Petrisor I and Negrea M 2005 *Plasma Phys. Control. Fusion* **47** 2145
[13] Negrea M and Petrisor I 2006 *Physics AUC* **16** 28
[14] Negrea M, Petrisor I and Weyssow B 2007 *Plasma Phys. Control. Fusion* **49** 1767
[15] Petrisor I, Negrea M and Weyssow B 2007 *Phys. Scr.* **75** 1
[16] Negrea M, Petrisor I and Constantinescu D 2010 *Rom. J. Phys.* **55** 1013
[17] Petrisor I and Negrea M 2012 *Physics AUC* **22** 68
[18] Negrea M, Petrisor I and Constantinescu D 2014 *Physics AUC* **24** 116
[19] Negrea M, Petrisor I and Weyssow B 2008 *J. Optoelectron. Adv. Mater.* **10** 1942
[20] Negrea M, Petrisor I and Weyssow B 2008 *Phys. Scr.* **77** 055502
[21] Negrea M, Petrisor I and Weyssow B 2008 *J. Optoelectron. Adv. Mater.* **10** 1946
[22] Shalchi A, Negrea M and Petrisor I 2016 *Phys. Plasmas* **23** 072306
[23] Negrea M, Petrisor I and Shalchi A 2017 *Phys. Plasmas* **24** 112303
[24] Pometescu N, Negrea M and Rotaru P 1998 *Plasma Phys. Control. Fusion* **40** 1383
[25] Steinbrecher G *et al* 1997 *Plasma Phys. Control. Fusion* **39** 2039
[26] Petrisor I *et al* 2012 *Proceedings of the 2012 International Conference on High Performance Computing and Simulation, HPCS* **6266983** 623–7
[27] Horton W 1985 *Plasma Phys. Contr. Fusion* **27** 937
[28] Weyssow B, Misguich J H and Balescu R 1991 *Plasma Phys. Control. Fusion* **33** 763
[29] Balescu R 2005 *Aspects on Anomalous Transport in Plasmas* (Bristol: Institute of Physics Publishing)
[30] Negrea M *et al* 2011 *Plasma Phys. Control. Fusion* **53** 085022
[31] Scott B D 2002 *New J. Phys.* **4** 52.1
[32] Wesson J 1997 *Tokamaks* 2nd edn (New Year: Oxford University Press)
[33] Giroud C *et al* (the JET EFDA Contributors) 2007 *Nucl. Fusion* **47** 313
[34] Cimpoiasu R 2017 *J. Nonlinear Math. Phys.* **24** 531
[35] Cimpoiasu R 2014 *Phys. Plasmas* **21** 042118
[36] Negrea M 2019 *Plasma Phys. Control. Fusion* **61** 065004